

Passive scalar transport in shear-flow turbulence

Enikő J. M. Madarassy¹ and Axel Brandenburg^{1,2}

¹*NORDITA, AlbaNova University Center, Roslagstullsbacken 23, SE-10691 Stockholm, Sweden*

²*Department of Astronomy, AlbaNova University Center, Stockholm University, SE 10691 Stockholm, Sweden*

(Dated: June 21, 2024, Revision: 1.14)

The turbulent diffusivity tensor is determined for linear shear flow turbulence using numerical simulations. For moderately strong shear, the diagonal components are found to increase quadratically with Peclet and Reynolds numbers until they become constant value at larger values. The diffusivity tensor is found to have components proportional to the symmetric and antisymmetric parts of the velocity gradient matrix, as well as products of these. All components decrease with the wavenumber of the mean field in a Lorentzian fashion. The components of the diffusivity tensor do not significantly depend on the presence of helicity in the turbulence.

PACS numbers: PACS Numbers : 47.27.tb, 47.27.ek, 95.30.Lz

INTRODUCTION

Turbulent diffusion quantifies the effective exchange of chemicals in a turbulent medium. If there is a gradient in the mean concentration \bar{C} of chemicals, there will be a net mean flux $\bar{\mathcal{F}} = \bar{u}\bar{C}$ of chemicals resulting from a systematic correlation of fluctuations in the concentration c and the turbulent velocity \mathbf{u} . This mean flux will be down the gradient of concentration, with

$$\bar{\mathcal{F}} = -\kappa_t \nabla \bar{C}, \quad (1)$$

where κ_t is the turbulent diffusivity. However, modifications are expected when the turbulence is anisotropic. In that case this relation takes the form

$$\bar{\mathcal{F}}_i = -\kappa_{ij} \nabla_j \bar{C}, \quad (2)$$

where κ_{ij} is now the turbulent diffusion tensor. In this paper we are interested in the anisotropy caused by the presence of shear. One of the results one expects to see is a suppression of turbulent transport in the cross-stream direction. This effect is discussed in various physical circumstances such as geophysical flows [1], turbulent plasmas [2], and solar physics [3, 4].

Much of this research is done using analytic techniques such as the first-order smoothing approximation and the renormalization group analysis. However, in recent years it has become possible to calculate turbulent transport coefficients using numerical realizations of turbulence from direct simulations. Turbulent transport coefficients can then be determined by imposing a gradient in the passive scalar concentration and measuring the resulting concentration fluxes [5]. By imposing gradients in three different directions it is possible to assemble all components of the turbulent diffusion tensor.

In recent years such a technique has been applied to the case of magnetic fields whose evolution is controlled not just by turbulent magnetic diffusion, but also by non-diffusive contributions known as the α effect [6, 7]. In this way it has been possible to investigate numerically the effects of shear and rotation in regimes that cannot be treated analytically. The technique is known under the name test-field method, which refers

to the fact that this approach involves the analysis of correlations for a set of different pre-determined test fields. In the analogous case of passive scalars, this method is now often referred to as test-scalar method [8].

Using this method, it has recently been possible to determine the turbulent diffusion tensor in cases where the turbulence is anisotropic owing to the presence of either rotation or an imposed magnetic field [8]. In the case of rotation the angular velocity vector $\boldsymbol{\Omega}$ provides a new element for constructing an anisotropic rank-2 tensor of the form [9]

$$\kappa_{ij} = \kappa_0 \delta_{ij} + \kappa_\Omega \epsilon_{ijk} \hat{\Omega}_k + \kappa_{\Omega\Omega} \hat{\Omega}_i \hat{\Omega}_j, \quad (3)$$

where $\hat{\Omega} = \boldsymbol{\Omega}/|\boldsymbol{\Omega}|$ is the unit vector along the rotation axis and κ_0 , κ_Ω , and $\kappa_{\Omega\Omega}$ are functions of the flow parameters. Note that $\boldsymbol{\Omega}$ is a pseudo vector while κ_{ij} is a proper tensor, so all three coefficients in Eq. (3) are proper scalars. In the case of a shear flow, an obvious possible ansatz is obtained by replacing $\boldsymbol{\Omega}$ by the vorticity $\bar{\mathbf{W}} = \nabla \times \bar{\mathbf{U}}$, which is also a pseudo (or axial) vector, and $\bar{\mathbf{U}}$ is the mean shear flow. However, such an ansatz would be incomplete, because it only captures the antisymmetric part of the velocity gradient matrix $\bar{U}_{i,j}$, where a comma denotes partial differentiation. A more natural approach would therefore be to invoke both symmetric and antisymmetric parts of the velocity gradient matrix by writing it as $\bar{U}_{i,j} = \bar{S}_{ij} + \bar{A}_{ij}$, where

$$\bar{S}_{ij} = \frac{1}{2}(\bar{U}_{i,j} + \bar{U}_{j,i}), \quad (4)$$

$$\bar{A}_{ij} = \frac{1}{2}(\bar{U}_{i,j} - \bar{U}_{j,i}). \quad (5)$$

The latter can also be written as $\bar{A}_{ij} = -\frac{1}{2}\epsilon_{ijk}\bar{W}_k$. A proper rank-2 tensor can then be expressed as

$$\kappa_{ij} = \kappa_t \delta_{ij} + \kappa_S \bar{S}_{ij} + \kappa_A \bar{A}_{ij} + \kappa_{SS} (\bar{\mathbf{S}}\bar{\mathbf{S}})_{ij} + \kappa_{AS} (\bar{\mathbf{A}}\bar{\mathbf{S}})_{ij}, \quad (6)$$

where κ_t , κ_S , κ_A , κ_{SS} , and κ_{AS} are proper scalars that are again functions of the flow parameters. An important goal of this work is to determine these coefficients for a linear shear flow of the form

$$\bar{\mathbf{U}} = (0, Sx, 0), \quad (7)$$

where $S = \text{const}$ is the shear rate, which is not to be confused with the tensor \mathbf{S} . For a linear shear flow given by Eq. (7), the tensors \mathbf{S} and \mathbf{A} are constants, and their only non-vanishing components are

$$\bar{S}_{xy} = \bar{S}_{yx} = -\bar{A}_{xy} = \bar{A}_{yx} = S/2. \quad (8)$$

Note also that

$$\bar{\mathbf{S}}^2 = -\bar{\mathbf{A}}^2 = (S/2)^2 \text{diag}(1, 1, 0), \quad (9)$$

$$\bar{\mathbf{A}}\bar{\mathbf{S}} = -\bar{\mathbf{S}}\bar{\mathbf{A}} = (S/2)^2 \text{diag}(-1, 1, 0). \quad (10)$$

With these preparations we can now express all 9 components of κ_{ij} in terms of the 5 coefficients in Eq. (6) as follows:

$$\kappa_{11} = \kappa_t + \frac{1}{4}S^2(\kappa_{SS} - \kappa_{AS}), \quad (11)$$

$$\kappa_{22} = \kappa_t + \frac{1}{4}S^2(\kappa_{SS} + \kappa_{AS}), \quad (12)$$

$$\kappa_{33} = \kappa_t, \quad (13)$$

$$\kappa_{12} = \frac{1}{2}S(\kappa_S - \kappa_A), \quad (14)$$

$$\kappa_{21} = \frac{1}{2}S(\kappa_S + \kappa_A). \quad (15)$$

Given that all 9 components of κ_{ij} can be determined from simulation data using the test-scalar method, we can use the five relations above to compute the five unknown coefficients in Eq. (6) via

$$\kappa_S S = \kappa_{21} + \kappa_{12}, \quad \kappa_A S = \kappa_{21} - \kappa_{12}, \quad (16)$$

$$\kappa_{SS} S^2/2 = \kappa_{22} + \kappa_{11} - 2\kappa_{33}, \quad (17)$$

$$\kappa_{AS} S^2/2 = \kappa_{22} - \kappa_{11}, \quad (18)$$

$$\kappa_t = \kappa_{33}. \quad (19)$$

Note that combinations such as $\kappa_S S$ and $\kappa_{SS} S^2/2$ have still the same dimension as κ_{ij} , so in the following we shall quote these combinations in that form.

In principle it is possible to construct κ_{ij} using also the velocity vector $\bar{\mathbf{U}}$ itself. However, $\bar{\mathbf{U}}$ varies in x and vanishes at $x = 0$. On the other hand, we expect the components of κ_{ij} not to depend explicitly on position, making a construction in terms of $\bar{\mathbf{U}}$ less favorable. Furthermore, the tensor $\bar{U}_i \bar{U}_j$, which has only one component in the yy position, can already be constructed from $\bar{\mathbf{S}}^2 - \bar{\mathbf{A}}\bar{\mathbf{S}} = \text{diag}(0, 2, 0)$, so no new information would be added. However, this changes when we also admit helical turbulent flows, because then there could be tensors of the form $\bar{W}_i \bar{U}_j$ and $\bar{W}_i \bar{U}_j$ which have components in the yz and zy directions. For this reason we shall also investigate helical turbulence in some cases.

A comment regarding the case of rotation is here in order. In hindsight it might have been more natural to write Eq. (3) in terms of the antisymmetric matrix $\bar{A}_{ij} = -\epsilon_{ijk} \hat{\Omega}_k$, i.e.

$$\kappa_{ij} = \kappa_t^\Omega \delta_{ij} + \kappa_A^\Omega \bar{A}_{ij} + \kappa_{AA}^\Omega (\bar{\mathbf{A}}^2)_{ij}, \quad (20)$$

with coefficients that are related to those in Eq. (3) via

$$\kappa_t^\Omega = \kappa_0 + \kappa_{\Omega\Omega}, \quad \kappa_A^\Omega = -\kappa_\Omega, \quad \kappa_{AA}^\Omega = \kappa_{\Omega\Omega}. \quad (21)$$

Evidently, this representation is equivalent to that of Eq. (3).

In the rest of this paper we continue with the case of a pure shear flow. The aim is to determine the coefficients in Eq. (6) as functions of flow parameters such as the Peclet number and the shear parameter.

SIMULATIONS

We simulate turbulence by solving the compressible hydrodynamic equations with an imposed random forcing term and an isothermal equation of state, so that the pressure p is related to ρ via $p = \rho c_s^2$, where c_s is the isothermal sound speed. We consider a periodic Cartesian domain of size L^3 . In the presence of shear the hydrodynamic equations for ρ and the departure \mathbf{U} from the imposed shear flow $\bar{\mathbf{U}}$ take the form,

$$\frac{D \ln \rho}{Dt} = -\nabla \cdot \mathbf{U}, \quad (22)$$

$$\frac{D\mathbf{U}}{Dt} = -S\mathbf{U}_x \hat{\mathbf{y}} - c_s^2 \nabla \ln \rho + \mathbf{f} + \mathbf{F}_{\text{visc}}, \quad (23)$$

where $D/Dt = \partial/\partial t + (\mathbf{U} + \bar{\mathbf{U}}) \cdot \nabla$ is the advective derivative with respect to the full velocity, $\mathbf{F}_{\text{visc}} = \rho^{-1} \nabla \cdot 2\rho\nu\mathbf{S}$ is the viscous force, ν is the kinematic viscosity, $S_{ij} = \frac{1}{2}(U_{i,j} + U_{j,i}) - \frac{1}{3}\delta_{ij} \nabla \cdot \mathbf{U}$ is the traceless rate of strain tensor, and \mathbf{f} is a random forcing function consisting of plane transversal waves with random wavevectors \mathbf{k} such that $|\mathbf{k}|$ lies in a band around a given forcing wavenumber k_f . The vector \mathbf{k} changes randomly from one timestep to the next. We have carried out simulations with helical and nonhelical forcing using the modified forcing function

$$\mathbf{f}_{\mathbf{k}} = \mathbf{R} \cdot \mathbf{f}_{\mathbf{k}}^{(\text{nohel})} \quad \text{with} \quad R_{ij} = \frac{\delta_{ij} - i\sigma\epsilon_{ijk}\hat{k}_k}{\sqrt{1 + \sigma^2}}, \quad (24)$$

where $\mathbf{f}_{\mathbf{k}}^{(\text{nohel})}$ is the non-helical forcing function. In the helical case ($\sigma = \pm 1$) we recover the forcing function used in Ref. [10], and in the non-helical case ($\sigma = 0$) this forcing function becomes equivalent to that used in Ref. [11]. The forcing amplitude is chosen such that the Mach number $\text{Ma} = u_{\text{rms}}/c_s$ is about 0.1. We use triply-periodic boundary conditions, except that the x direction is shearing-periodic, i.e.

$$\mathbf{U}(-\frac{1}{2}L, y, z, t) = \mathbf{U}(\frac{1}{2}L, y + LSt, z, t), \quad (25)$$

where L is the side length of the cubic domain. This condition is routinely used in numerical studies of shear flows in Cartesian geometry [12, 13].

The test scalar equation is obtained by subtracting the averaged passive scalar equation from the original one and applying it to a predetermined set of six different mean fields,

$$\overline{C}^{ic} = C_0 \cos kx_i, \quad \overline{C}^{is} = C_0 \sin kx_i, \quad (26)$$

where x_i denotes x , y , and z for $i = 1, \dots, 3$, and C_0 is a normalization factor. The overbars denote planar averaging over the directions that are perpendicular to the direction in which the mean field varies. For each test field \overline{C}^{pq} we obtain a separate evolution equation for the corresponding fluctuating component c^{pq} ,

$$\frac{\partial c^{pq}}{\partial t} = -\nabla \cdot (\overline{\mathbf{U}} c^{pq} + \mathbf{u} \overline{C}^{pq} + \mathbf{u} c^{pq} - \overline{\mathbf{u} c^{pq}}) + \kappa \nabla^2 c^{pq}, \quad (27)$$

where κ is the microscopic (molecular) passive scalar diffusivity, $p = 1, \dots, 3$, and $q = c$ or s . In this way, we calculate six different fluxes, $\overline{\mathcal{F}}^{pq} = \overline{\mathbf{u} c^{pq}}$, and compute the 9 relevant components of κ_{ij}

$$\kappa_{ij} = -\langle \cos kx_j \overline{\mathcal{F}}_i^{js} - \sin kx_j \overline{\mathcal{F}}_i^{jc} \rangle / k, \quad (28)$$

for $i, j = x, y, z$. Here, angular brackets denote volume averages. In this paper we present the values of κ_{ij} in non-dimensional form by normalizing with

$$\kappa_{t0} = u_{\text{rms}} / 3k_f, \quad (29)$$

which is the expected value for large values of Pe .

Our simulations are characterized by two important non-dimensional control parameters, the shear parameter Sh and the Peclet number Pe , defined as

$$\text{Sh} = S / (u_{\text{rms}} k_f), \quad \text{Pe} = u_{\text{rms}} / (\kappa k_f), \quad (30)$$

In addition, there is the Schmidt number $\text{Sc} = \nu / \kappa$, but we keep it equal to unity in all cases reported below. Note also that in most cases we use negative values of S , so we have $\text{Sh} < 0$. The smallest wavenumber that fits into the computational domain is $k_1 = 2\pi/L$. We choose the forcing wavenumber to be 3 times larger, i.e. $k_f/k_1 = 3$.

The simulations have been carried out using the PENCIL CODE [19] which is a high-order finite-difference code (sixth order in space and third order in time) for solving the compressible hydrodynamic equations. The test-scalar equations were already implemented into the public-domain code, but have now been generalized to determining all 9 components of κ_{ij} . The numerical resolution used in the simulations depends on the Peclet number and reaches 128^3 meshpoints for runs with $\text{Pe} \approx 120$. In this paper we restrict ourselves to time spans short enough so that the so-called vorticity dynamo has no time to develop; see Refs. [14, 15] for details.

RESULTS

Dependence on the shear parameter

We begin by discussing the dependence of the coefficients in Eq. (6) on the shear parameter Sh . The result is shown in Fig. 1. It turns out that all five coefficients are positive. We find that $\kappa_t = \text{const} = 2$ for non-helical turbulence and 3 for helical turbulence, independent of the value of shear provided $\text{Sh} < 0.5$. The other coefficients show the following approximate scaling behavior:

$$\kappa_S S \approx 5\text{Sh}, \quad \kappa_{SS} S^2 / 2 \approx 30\text{Sh}^2, \quad (31)$$

$$\kappa_A S \approx 10\text{Sh}^3, \quad \kappa_{AS} S^2 / 2 \approx 40\text{Sh}^3. \quad (32)$$

The fact that κ_A and κ_{AS} scale with the third power of Sh suggests that these are higher order effects that are not easily captured by perturbative approaches.

Dependence on Peclet number

We have performed simulations for different values of the Peclet number and have determined the coefficients in Eq. (6) for each simulation. It turns out that the first four coefficients can well be approximated by simple algebraic functions,

$$\kappa_t = \frac{2\kappa_{\text{Sh}} \text{Pe}^2}{\text{Pe}_0^2 + \text{Pe}^2}, \quad \kappa_S S = \frac{\kappa_{\text{Sh}} \text{Pe}^3}{(\text{Pe}_0^2 + \text{Pe}^2)^{3/2}}, \quad (33)$$

$$\kappa_{SS} S^2 / 2 = \frac{\kappa_{\text{Sh}} \text{Pe}^4}{(\text{Pe}_0^2 + \text{Pe}^2)^2}, \quad \kappa_A S = \frac{\kappa_{\text{Sh}} \text{Pe}^4}{(\text{Pe}_0^2 + \text{Pe}^2)^{2.4}}, \quad (34)$$

where $\kappa_{\text{Sh}} = 0.95\kappa_{t0}$ and $\text{Pe}_0 = 3.8$ are fit parameters. In the case of κ_{AS} the error bars are so large that no conclusive statements can be made.

In Fig. 2 we have also shown results for cases where the forcing function has maximum helicity. No significant dependence can be seen, except for κ_t which is slightly enhanced in the helical case with weak shear. This suggests that this dependence is not connected with the presence of shear.

In Fig. 3 we show the dependence of the diagonal components of κ_{ij} on Pe . Over the range of parameters shown here, the difference between the three components is small, although there is a tendency for κ_{yy} to be somewhat enhanced around $\text{Pe} = 20$, while κ_{zz} is slightly smaller than κ_{xx} .

Wavenumber dependence

We consider now the dependence of the diagonal components of κ_{ij} on the wavenumber k of the test scalar in Eq. (26). A dependence of κ_{ij} on k reflects the fact that there is poor scale separation, i.e. k/k_f is not very small. In such a case, the

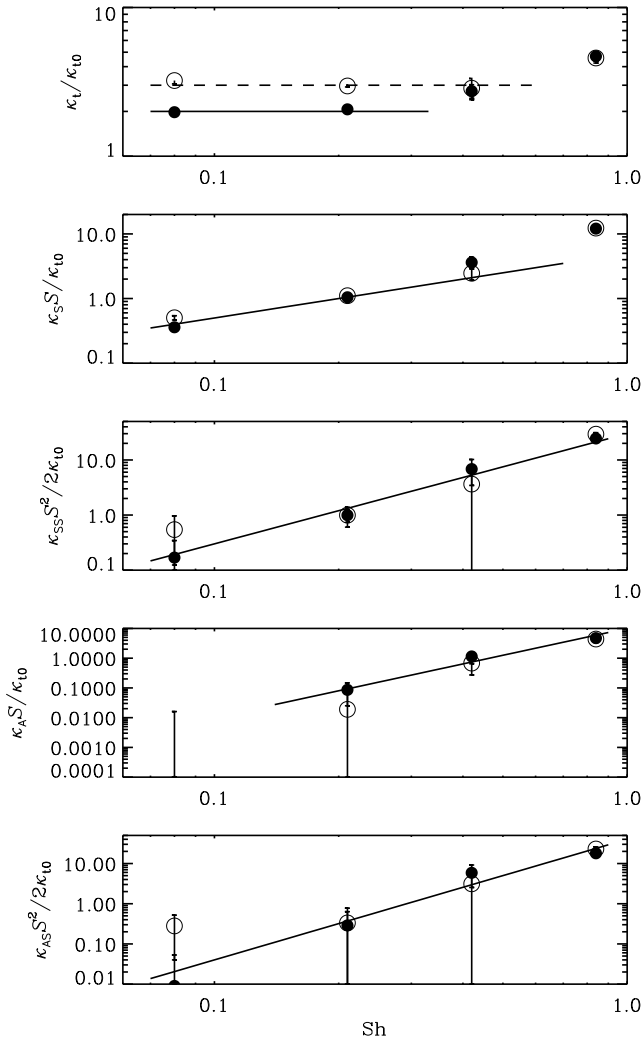


FIG. 1: Dependence of the coefficients in Eq. (6) on Sh for $Pe = 25$. Dependence on Sh for cases with helicity (dashed lines) and without (solid lines).

multiplication with a turbulent diffusivity in Eqs. (1) and (2) must be replaced by a convolution with an integral kernel [8]. In Fourier space the convolution corresponds to a multiplication. The full integral kernel can be assembled by determining the full k dependence and then Fourier transforming back into real space.

The resulting dependence on k is shown in Fig. 4 for two values of the shear parameter. In agreement with earlier findings, the components of κ_{ij} show a Lorentzian dependence on k , i.e.

$$\kappa_{ij} = \frac{\kappa_{ij}^{(0)}}{1 + (ak/k_{\xi})^2}, \quad (35)$$

where $a \approx 0.2$ for the κ_{11} and κ_{22} components, and $a \approx 0.4$ for the κ_{33} component. Here, $\kappa_{ij}^{(0)}$ is the value for $k = 0$, which is approximately equal to κ_{t0} , defined in Eq. (29).

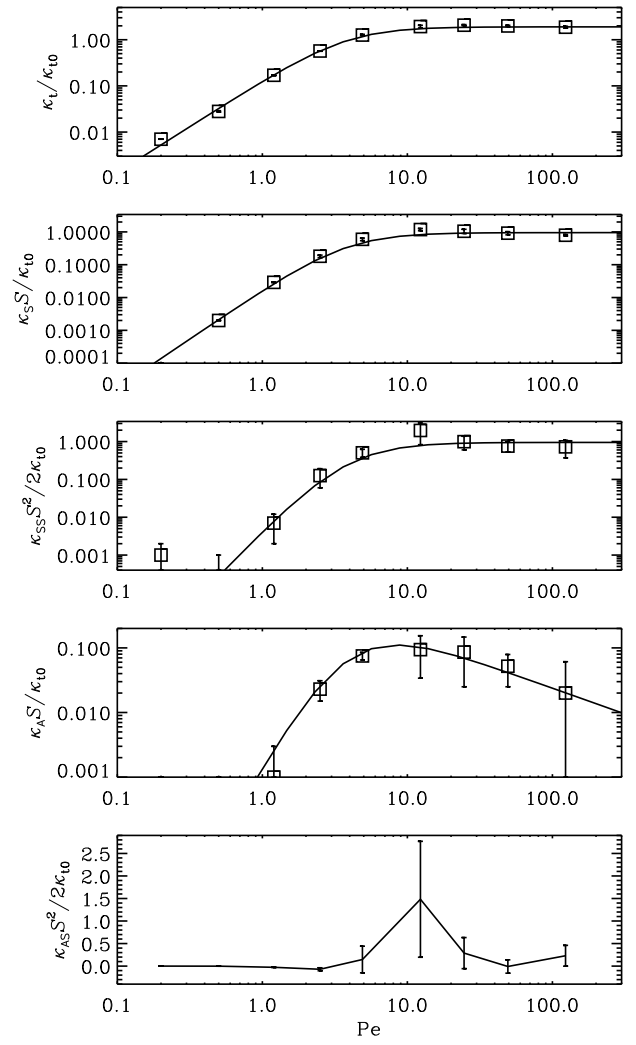


FIG. 2: Dependence of the coefficients in Eq. (6) on Pe for $Sh = -0.2$. The symbols give the numerical results and the solid lines represent fits given by Eqs. (33) and (34). The dashed line in the first panel is for a run with maximum helicity. All runs with helicity are marked with open symbols.

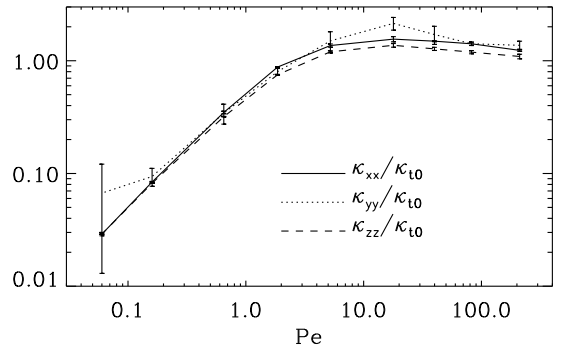


FIG. 3: Dependence of the diagonal components of κ_{ij} on Pe .

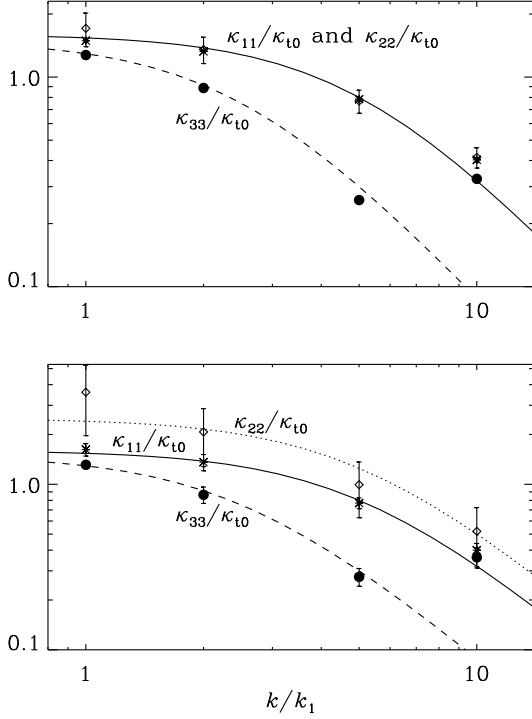


FIG. 4: Dependence of the diagonal components of κ_{ij} on k for $\text{Sh} = -0.13$ (upper panel) and $\text{Sh} = -0.20$ (lower panel).

Effects of helicity

As discussed in the introduction, the presence of helicity allows one in principle to construct proper tensors proportional to $\overline{W}_i \overline{U}_j$ and $\overline{W}_j \overline{U}_i$, because we have now access to a pseudoscalar given by the kinetic helicity of the turbulence. If this does indeed have an effect, one would expect there to be finite yz and zy components. In Fig. 5 we see that there is no evidence for this to be the case.

EXPECTATIONS FROM THE τ APPROXIMATION

In this section we give the results for κ_{ij} using the pressureless τ approximation. In this approach one considers the evolution equation for $\overline{\mathcal{F}}$,

$$\frac{\partial \overline{\mathcal{F}}_i}{\partial t} = \overline{u_i c} + \overline{u_i \dot{c}}, \quad (36)$$

where dots denote time derivatives [5, 16]. We use Eqs. (23) and (27), ignore the pressure term, assume $\overline{\mathbf{f}}_c = 0$, and obtain

$$\overline{u_i c} = -S \delta_{i2} \delta_{1k} \overline{u_k c} + \text{triple correlations}, \quad (37)$$

$$\overline{u_i \dot{c}} = -\overline{u_i u_j} \nabla_j \overline{C} + \text{triple correlations}. \quad (38)$$

The triple correlation terms result from the nonlinearities in the evolution equations Eqs. (23) and (27). In the τ approximation we substitute the sum of the triple correlations

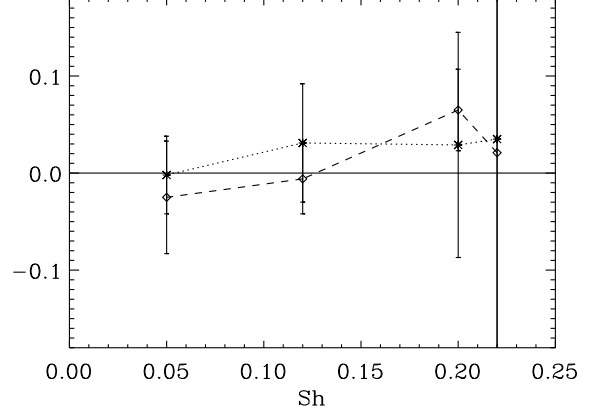


FIG. 5: Plot of κ_{yz} (dotted) and κ_{zy} (dashed) versus Sh for maximally helical turbulence. No significant dependence can be seen.

by quadratic correlations, i.e. in the present case by $-\overline{u_i c}/\tau$ [17, 18]. We write the resulting equation in matrix form,

$$\tau \frac{\partial \overline{\mathcal{F}}_i}{\partial t} = -\mathbf{L}_{ik} \overline{\mathcal{F}}_k - \tau \overline{u_i u_j} \nabla_j \overline{C}, \quad (39)$$

where $\mathbf{L}_{ik} = \delta_{ik} + S\tau \delta_{i2} \delta_{1k}$. We solve this equation for $\overline{\mathcal{F}}$ and obtain

$$\overline{\mathcal{F}}_i = -(\mathbf{L}^{-1})_{ij} \left(\tau \overline{u_j u_k} \nabla_k \overline{C} + \tau \frac{\partial \overline{\mathcal{F}}_i}{\partial t} \right), \quad (40)$$

where $(\mathbf{L})_{ik}^{-1} = \delta_{ik} - \text{Sh} \delta_{i2} \delta_{1k}$ with $\text{Sh} = S\tau$. In the presence of shear, the Reynolds stress tensor $\overline{u_j u_k}$ is no longer diagonal, but it has finite xy and yx components. In the following we represent $\overline{u_j u_k}$ in the form

$$\overline{\mathbf{u}\mathbf{u}} = \overline{u_x^2} \begin{pmatrix} 1 & -\delta & 0 \\ -\delta & 1 + \epsilon & 0 \\ 0 & 0 & 1 + \epsilon_z \end{pmatrix}. \quad (41)$$

The dependence of δ and ϵ on Sh is shown in Fig. 6, while ϵ_z is found to be small.

Inserting this expression in Eq. (40) we obtain

$$\frac{\kappa}{\kappa_{t0}} = \begin{pmatrix} 1 & -\delta & 0 \\ -\delta - \text{Sh} & 1 + \epsilon + \delta \text{Sh} & 0 \\ 0 & 0 & 1 + \epsilon_z \end{pmatrix}. \quad (42)$$

In the stationary state we may ignore the time derivative and recover Eq. (3) with

$$\frac{\kappa_{SS} S}{\kappa_{t0}} = -2\delta - \text{Sh}, \quad \frac{\kappa_{AS} S}{\kappa_{t0}} = -\text{Sh}, \quad (43)$$

$$\frac{\kappa_{SS} S^2/2}{\kappa_{t0}} + 2\epsilon_z = \frac{\kappa_{AS} S^2/2}{\kappa_{t0}} = \epsilon - \delta \text{Sh}. \quad (44)$$

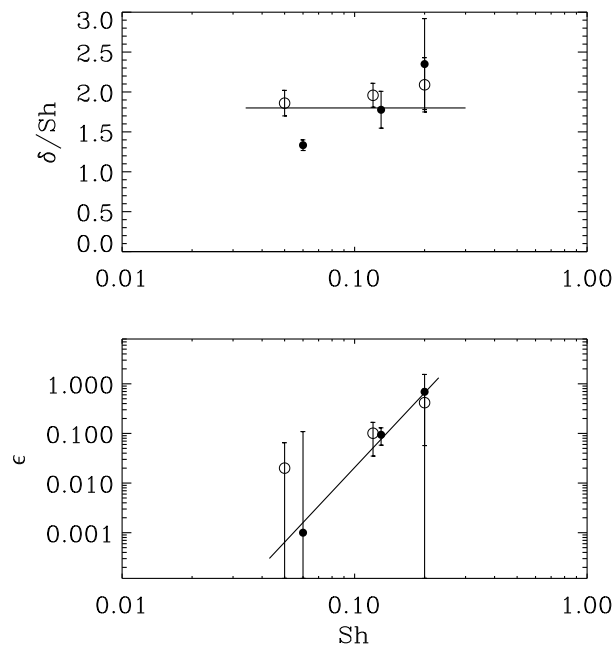


FIG. 6: Dependence of δ and ϵ on Sh for nonhelical turbulence (solid symbols) and helical turbulence (open symbols). The solid line in the second panel has slope 5.

We recall that Sh is negative, and that δ changes sign with Sh . Therefore we expect κ_S and κ_A to be positive, which agrees with the simulations. Furthermore, we expect κ_{yy} to be enhanced, which also agrees with the simulations. However, the slight suppression of κ_{zz} cannot be explained by the simple theory, because ϵ_z is small and perhaps even positive, suggesting at best an opposite trend.

CONCLUSIONS

The present work has shown that shear introduces anisotropies to the diffusivity tensor for passive scalar diffusion. These additional components are proportional to the even and odd parts of the velocity gradient tensor, as well as products of these tensors. Those components that are connected with the antisymmetric part of the velocity gradient tensor scale with the third power of the shear parameter, suggesting that these effects cannot be captured perturbatively.

In general, turbulent transport tends to be enhanced in the direction of the shear, i.e. κ_{yy} tends to be larger than κ_{xx} and κ_{zz} . Furthermore, κ_{zz} tends to be suppressed relative to κ_{xx} . This is a result that is not reproduced by the τ approximation.

In particular, there is no evidence for a suppression of turbulent transport in the cross-stream or x direction. Instead, there is a suppression in the direction out of the plane of the shear flow.

The transport properties are not affected by the presence of helicity. In other words, there is no evidence for the presence of tensor components proportional to $\overline{W}_i \overline{U}_j$ and $\overline{W}_j \overline{U}_i$.

We thank Alex Hubbard and Karl-Heinz Rädler for suggestions and simulating discussions. We acknowledge the use of computing time at the Center for Parallel Computers at the Royal Institute of Technology in Sweden. This work was supported in part by the European Research Council under the AstroDyn Research Project 227952 and the Swedish Research Council grant 621-2007-4064.

-
- [1] P. Terry, *Rev. Mod. Phys.* **72**, 109 (2000).
 - [2] K. Burrell, *Phys. Plasmas* **4**, 1499 (1997).
 - [3] E. Kim, *Astron. Astrophys.* **441**, 763 (2005).
 - [4] N. Leprovost and E. Kim, *Astron. Astrophys.* **456**, 617 (2006).
 - [5] A. Brandenburg, P. Käpylä, A. Mohammed, *Phys. Fluids* **16**, 1020 (2004).
 - [6] M. Schrunner, K.-H. Rädler, D. Schmitt, M. Rheinhardt, U. Christensen, *Astron. Nachr.* **326**, 245 (2005).
 - [7] M. Schrunner, K.-H. Rädler, D. Schmitt, M. Rheinhardt, U. Christensen, *Geophys. Astrophys. Fluid Dynam.* **101**, 81 (2007).
 - [8] A. Brandenburg, A. Svedin, G. M. Vasil, *Mon. Not. R. Astron. Soc.* **395**, 1599 (2009).
 - [9] L. L. Kitchatinov, G. Rüdiger, V. V. Pipin, *Astron. Nachr.* **315**, 157 (1994).
 - [10] A. Brandenburg, *Astrophys. J.* **550**, 824 (2001).
 - [11] N. E. L. Haugen, A. Brandenburg, and W. Dobler, *Astrophys. J.* **597**, L141 (2003).
 - [12] J. Wisdom, S. Tremaine, *Astronom. J.* **95**, 925 (1988).
 - [13] J. F. Hawley, C. F. Gammie, S. A. Balbus, *Astrophys. J.* **440**, 742 (1995).
 - [14] T. Elperin, N. Kleeorin, and I. Rogachevskii, *Phys. Rev. E* **68**, 016311 (2003).
 - [15] P. J. Käpylä, D. Mitra, and A. Brandenburg, *Phys. Rev. E* **79**, 016302 (2009).
 - [16] E. G. Blackman and G. B. Field, *Phys. Fluids* **15**, L73 (2003).
 - [17] S. I. Vainshtein and L. L. Kitchatinov, *Geophys. Astrophys. Fluid Dynam.* **24**, 273 (1983).
 - [18] N. I. Kleeorin, I. V. Rogachevskii, and A. A. Ruzmaikin, *Sov. Phys. JETP* **70**, 878 (1990).
 - [19] <http://pencil-code.googlecode.com/>